Mechanical and Pharmacological Activation of Piezo1 Channels Characterized by High Throughput Electrophysiology

Andrea Brüggemann[1], Nicoletta Murciano[1,2], Maria Giustina Rotordam[1], Markus Rapedius[1], Nadine Becker[1], Melanie J. Ludlow[3], Gregory Parsonage[3], Kevin Cuthbertson[3], Richard Foster[3], David J. Beech[3].

1 Nanion Technologies, Munich, Germany, 2 Theoretical Medicine and Biosciences, Saarland University, Homburg, Germany, 3 Univ Leeds, Leeds, United Kingdom.

Abstract

PIEZO channels are mechanically-activated cation channels that play important roles in biological functions including touch, proprioception, shear stress and stretch sensation as well as blood pressure regulation. Mutations in Homo sapiens PIEZO1 channels are associated with anemia, malarial resistance, lymphatic dysplasia and varicose vein disease, suggesting important red blood cells and vascular roles in humans.

The pharmacology of the PIEZO1 channels is in its infancy. Here we sought high throughput methodology for investigating small-molecule modulation in combination with mechanical stimulation.
A bottleneck in PIEZO drug development has been the lack of mechanical stimulation in automated patch clamp. Here we show how the optimization of pipetting parameters and the modification of the NPC-384 chip of the SyncroPatch 384 lead to the possibility to mechanically stimulate PIEZO1 channels using high throughput electrophysiology. Data of mouse and human PIEZO1 channels expressed in HEK T-REX 293 cells activated by either mechanical or chemical stimuli will be shown as well as the combination of both methods.

Under voltage-clamp we were able to show reliable quantification of PIEZO1 activation by fluid flow, Yoda1 (a small-molecule PIEZO1 agonist) and a Yoda1 analogue.

To our knowledge, this is the first time that mechanical stimulation of PIEZO channels in a high throughput planar patch clamp system has been shown. The possibility of comparing and combining mechanical and chemical stimulation in a high throughput electrophysiological assay facilitates the biophysical and pharmacological studies of PIEZO channels.

This work was supported by research grants from the Wellcome Trust, British Heart Foundation and has received funding from the European Union's Horizon 2020 research and innovation program.

Transient solution addition on the SyncroPatch 384

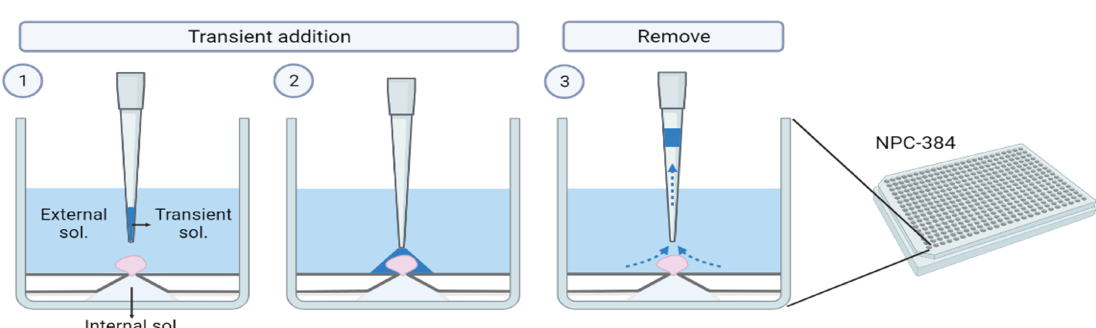

Figure 1: Transient solution addition on the SP384. Schematic illustration of a cross section of one well from NPC – 384 chips. The transient addition delivers a small volume of solution locally to the cell (**1** and **2**) and uses an aspiration step (**3**, dashed arrows) to recover the dispensed volume.

Effect of the position of the cell relative to the pipette

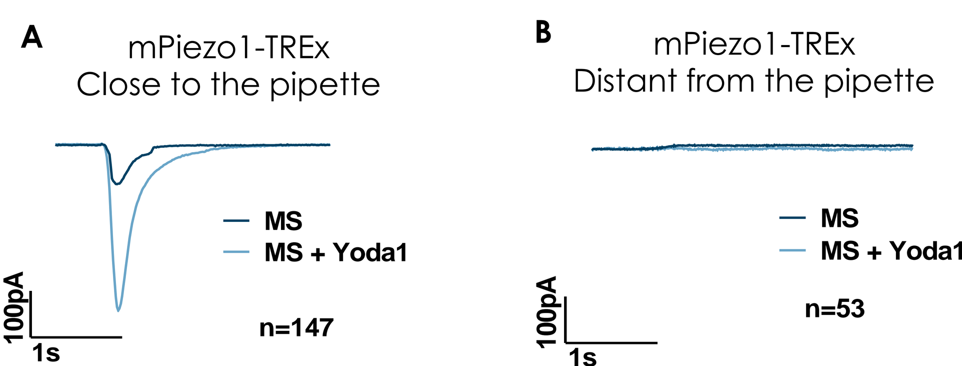

Figure 2: (**A**) The cell is close to the pipette. Averaged traces for PIEZO1-mediated currents activated by transient solution addition in the absence (MS) (dark blue traces) and presence of 10 µM Yoda1 (MS + Yoda1) (blue traces) from mPiezo1-TREx cells (n=147). (**B**) The cell is distant from the pipette. Averaged traces for PIEZO1-mediated activated by transient solution addition in the absence (MS) (dark blue traces) and presence of 10 µM Yoda1 (MS + Yoda1) (blue traces) from mPiezo1-TREx cells (n=53). Scale bars 100pA/1s for all the figures.

PIEZO1 currents activated by increasing pipetting speeds

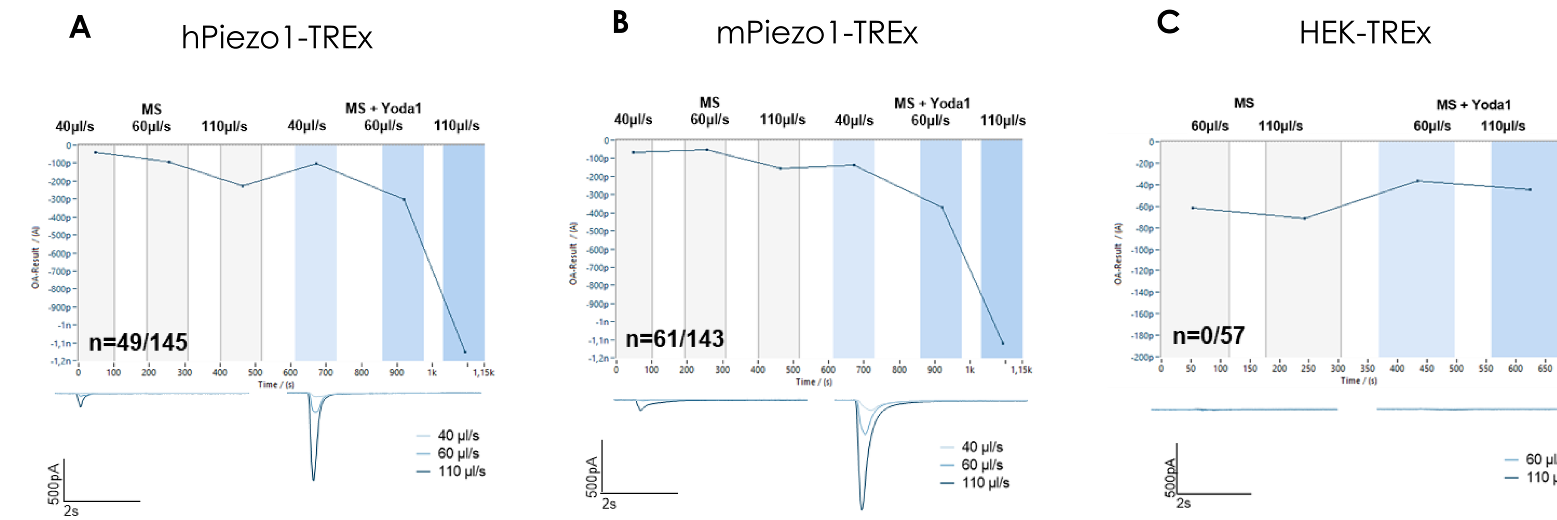

Figure 3: Averaged current values over time (top) of PIEZO1 activated by transient solution addition at three different pipetting speeds, 40 µl/s, 60 µl/s and 110 µl/s, for a total of six consecutive liquid additions in the absence (MS) (grey columns) and presence of 10 µM Yoda1 (MS + Yoda1) (light blue columns). Dots indicate current values from n averaged individual cells at the indicated pipetting speed. Averaged raw traces (bottom) activated by transient solution addition at three different pipetting speeds, 40 µl/s (light blue traces), 60 µl/s (blue traces) and 110 µl/s (dark blue traces), in the absence (MS) and presence of 10 µM Yoda1 (MS + Yoda1) from hPiezo1-TREx (n=49/145) (**A**), mPiezo1-TREx (n=61/143) (**B**), and HEK-TREx cells (n=0/57) (**C**). Scale bars 500pA/2s for all the figures.

Current density and percentage of responding cells evaluation at three different speeds of addition

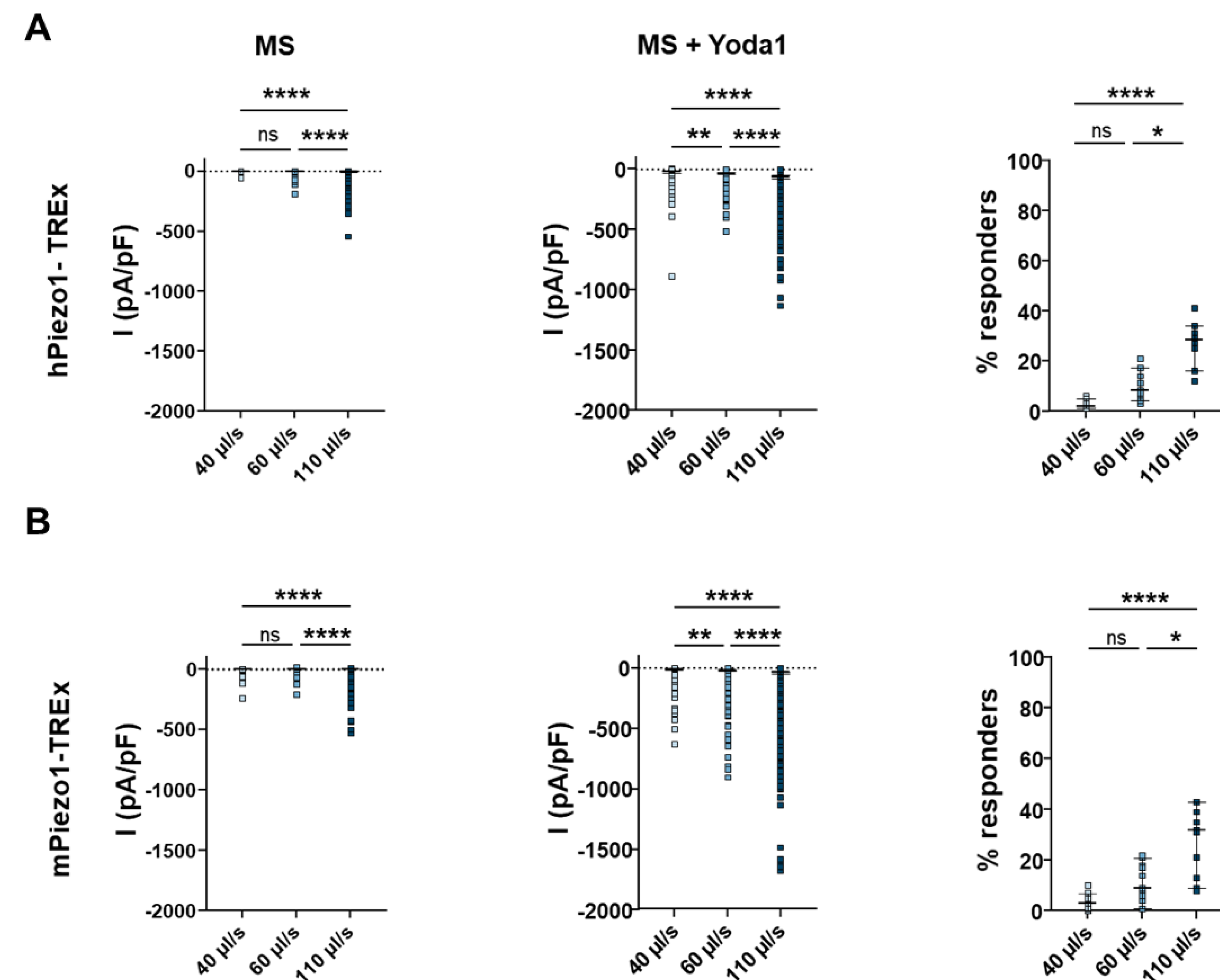

Figure 4: Current density values plotted against three different pipetting speeds, 40 µl/s (light blue squares), 60 µl/s (blue squares) and 110 µl/s (dark blue squares) elicited by MS only (**A**, **B left**) and in the presence of 10 µM Yoda1 (MS + Yoda1) (**A**, **B middle**) from hPiezo1-TREx (**A**) and mPiezo1-TREx cells (**B**). Each data point (square) represents the current density of a single cell. Data are shown as median with 95% CI indicated in black. Percentage of hPiezo1-TREx (N=10) (**A**, **right**) and mPiezo1-TREx cells (N=11) (**B**, **right**) responding to activation by MS +10 µM Yoda1 plotted against three different pipetting speeds. Each data point represents an independent experiment with median with 95% CI indicated in black. Multiple comparisons of median response magnitudes for all figures (**A**, **B**) were made using a Kruskal-Wallis ANOVA with Dunn's post-hoc test as the data did not fit a parametric distribution. (*p<0.05, **p<0.01, ****p<0,0001)
hPiezo1-TREx cells (40 µl/s n=108/1361; 60 µl/s n=242/1361; 110 µl/s n= 529/1361; N=10);
mPiezo1-TREx cells (40 µl/s n=120/1429; 60 µl/s n=230/1429; 110 µl/s n= 489/1429; N=11).

Correlation between currents elicited by MS and MS + Yoda1

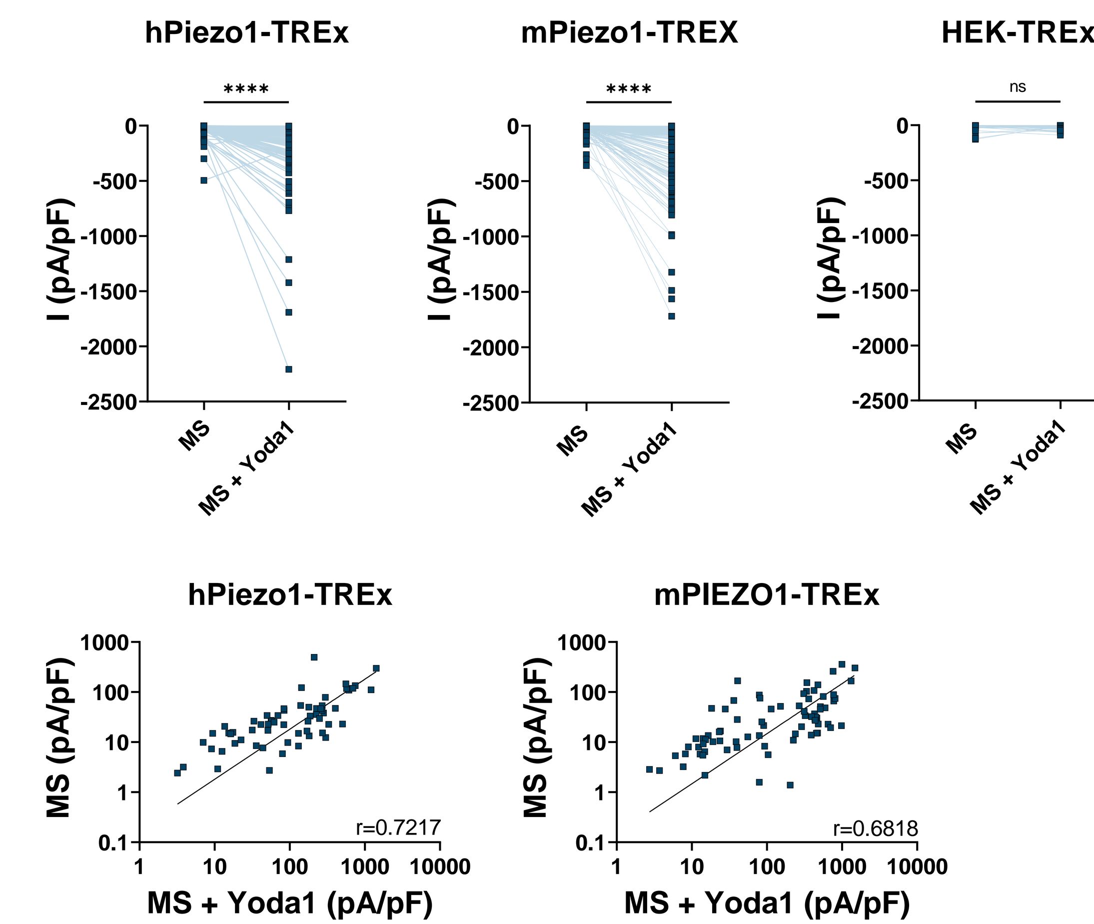

Figure 5: (**A**) Before-after charts comparing current density values elicited by MS and MS + Yoda1 at the maximum speed of 110 µl/s from hPiezo1-TREx (left) (n=209/758), mPiezo1-TREx (middle) (n=299/691) and HEK–TREx cells (right) (n=27/694), (N=15). Comparisons of median response magnitudes for all charts were made using Wilcoxon matched-pairs test as the data did not fit a parametric distribution. (****p<0,0001) (**B**) Scatter charts showing the correlation between current density values elicited by MS and MS + Yoda1 from hPiezo1-TREx (left) (n=61) and mPiezo1-TREx cells (right) (n=76). (hPiezo1-TREx, r=0,7217; mPiezo1-TREx, r=0,6818)

Percentage of responding cells at 110 µl/s speed

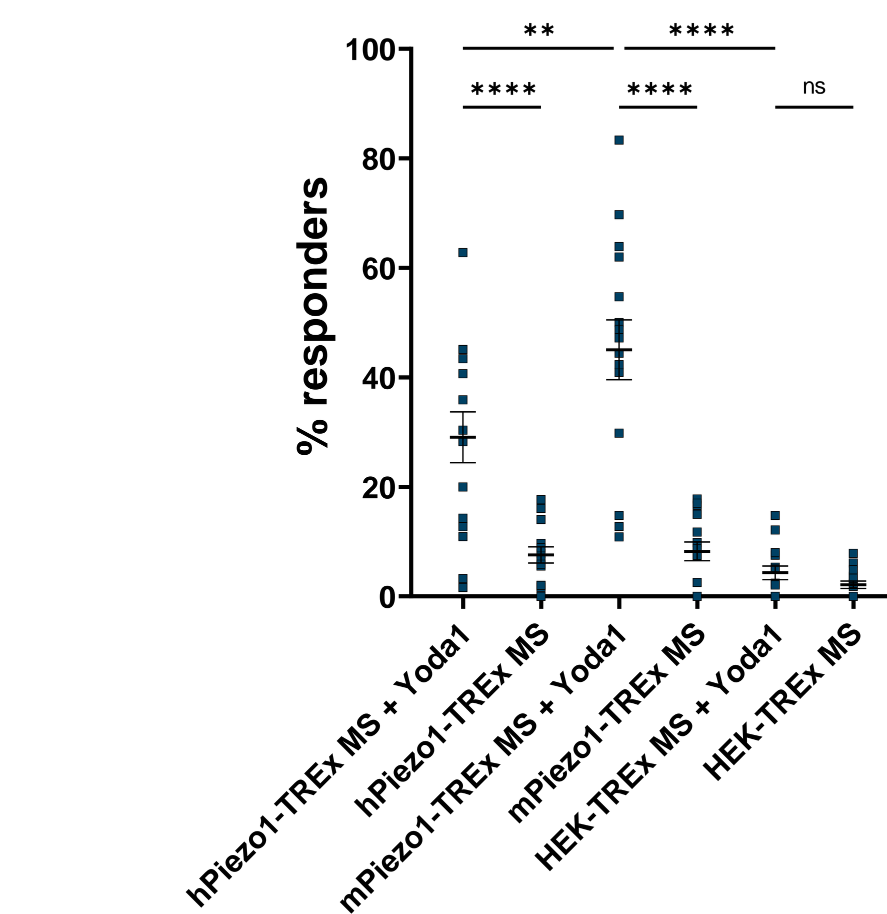

Figure 6: Percentage of hPiezo1-TREx (N=15), mPiezo1-TREx (N=15) and HEK-TREx cells (N=15) responding to activation by MS +10 µM Yoda1. Each data point represents an independent experiment with median with 95% CI indicated in black. Multiple comparisons of median response magnitudes were made using one-way ANOVA with Tukey's post-hoc test. (**p<0.01, ****p<0,0001)

Different pipetting volumes

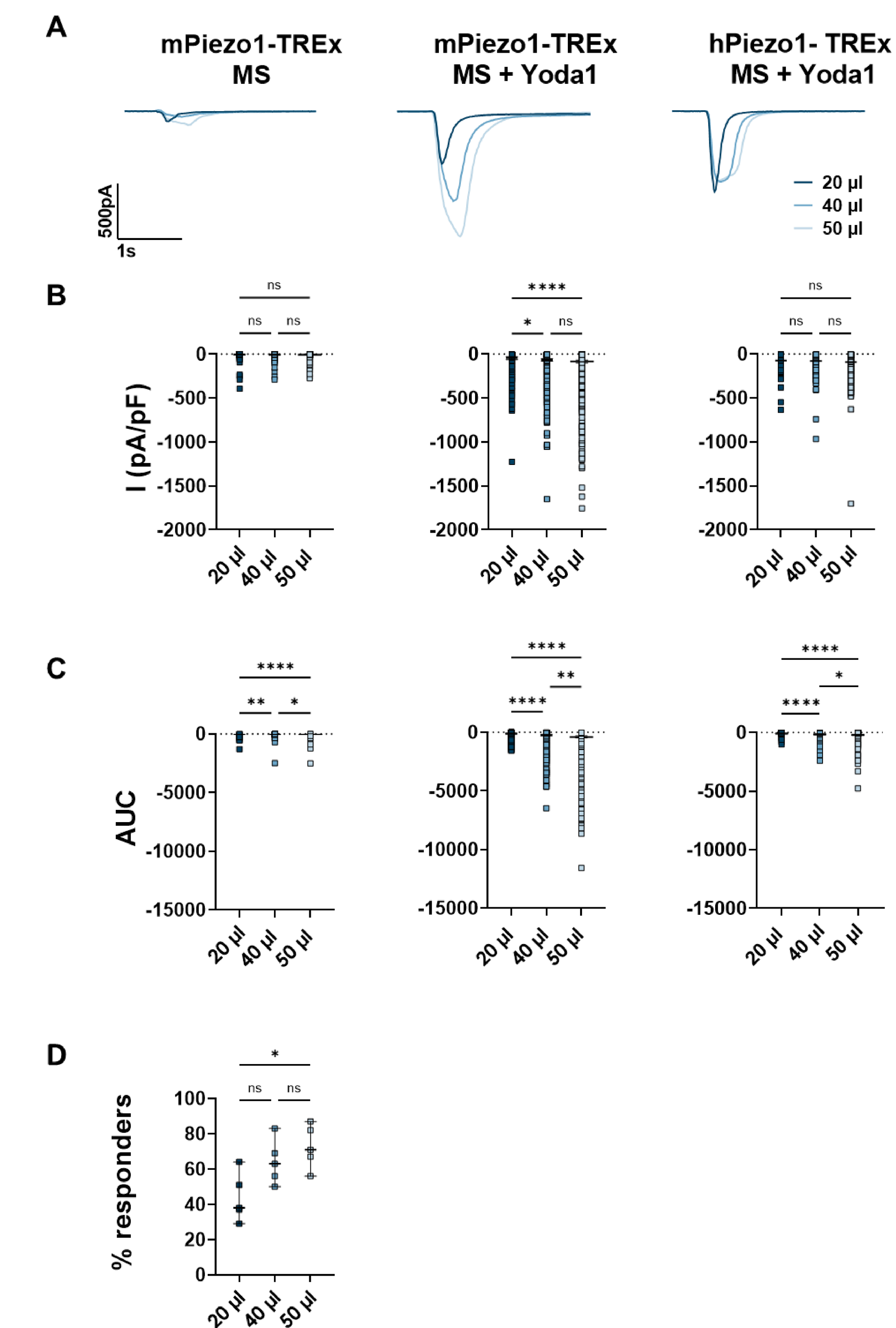

Figure 7: (**A**) Averaged raw traces activated by transient solution addition at 110 µl/s elicited by three different pipetting volumes, 20 µl (dark blue traces), 40 µl (blue traces) and 50 µl (light blue traces) in the absence (MS), (left) and presence of 10 µM Yoda1 (MS + Yoda1) (middle, right) from cells mPiezo-TREx cells (left, middle) (20 µl n=257/590; 40 µl n=378/590; 50 µl n=427/590; N=5) and hPiezo1-TREx cells (right) (20 µl n=222/645; 40 µl n=359/645; 50 µl n=420/645; N=5). Scale bars 500pA/1s. (**B**) Current density values and AUC values (**C**) plotted against three different pipetting volumes, 20 µl (dark blue squares), 40 µl (blue squares) and 50 µl (light blue squares) elicited by MS only (B left) and in the presence of 10 µM Yoda1 (MS + Yoda1) (B, middle, right) from mPiezo1-TREx cells (left, middle) and hPiezo1-TREx cells (right). Each data point (square) represents the current density or AUC of a single cell. Data are shown as median with 95% CI indicated in black. (**D**) Percentage of mPiezo1-TREx cells (N=5) responding to activation by MS +10 µM Yoda1 plotted against three different pipetting volumes. Each data point represents an independent experiment with median with 95% CI indicated in black. Multiple comparisons of median response magnitudes for all figures were made using a Kruskal-Wallis ANOVA with Dunn's post-hoc test as the data did not fit a parametric distribution. (*p<0.05, **p < 0.01, ****p<0,0001)

Discussion

In this study, we set out to develop an electrophysiological high-throughput approach to mechanically stimulate cells expressing the mechanosensitive ion channel PIEZO1 by using the SyncroPatch 384.

To optimize the mechanosensitive current response, we considered three parameters: 1) the position of the cells relative to the pipette tips, 2) the pipetting speed, and 3) the applied volume of solution.

The results show that it is possible to activate Piezo1 currents via mechanical stimulation and combine it with chemical stimulation as well.

We believe that this is a great starting point for a direct HTS assay for studying the Biophysical and chemical properties of mechano-sensitive channels.